Inorg. Chem. **2004**, *43*, 674–682

Structural Conversions of Molybdenum–Iron–Sulfur Edge-Bridged Double Cubanes and P^N-Type Clusters Topologically Related to the Nitrogenase P-Cluster

Yugen Zhang and R. H. Holm*

Department of Chemistry and Chemical Biology, Harvard University, Cambridge, Massachusetts 02138

Received August 13, 2003

Edge-bridged Mo–Fe–S double cubanes are versatile precursors for the synthesis of other clusters of the same nuclearity. Thus, the double cubane $[(Tp)_2Mo_2Fe_6S_8(PEt_3)_4]$ sustains terminal ligand substitution with retention of the $Mo_2Fe_6(\mu_3\text{-}S)_6(\mu_4\text{-}S)_2$ core structure and rearrangement to the $Mo_2Fe_6(\mu_2\text{-}S)_2(\mu_3\text{-}S)_6(\mu_6\text{-}S)$ topology of the nitrogenase P^N cluster upon reaction with certain nucleophiles. Four distinct processes for the conversion of double cubanes to P^N-type clusters are documented, affording the products $[(Tp)_2Mo_2Fe_6S_9(SR)_2]^{3-}$, $[(Tp)_2Mo_2Fe_6S_8(OMe)_3]^{3-}$, and $[(Tp)_2Mo_2Fe_6S_7(OMe)_4]^{2-}$. In the latter clusters, two methoxides are terminal ligands and one or two are μ_2-bridging ligands. The reverse transformation of a P^N-type cluster to an edge-bridged double cubane has been demonstrated by the reaction of $[(Tp)_2Mo_2Fe_6S_8(OMe)_3]^{3-}$ with Me_3SiX to afford $[(Tp)_2Mo_2Fe_6S_8X_4]^{2-}$ ($X = Cl^-$, Br^-). Edge-bridged double cubanes have been obtained in the oxidation states $[Mo_2Fe_6S_8]^{2+,3+,4+}$. The stable oxidation state of P^N-type clusters is $[Mo_2Fe_6S_9]^+$. Structures of five double cubanes and four P^N-type clusters are reported. The P^N-type clusters are synthetic representations of the biologically unique topology of the native P^N cluster. Best-fit superpositions of the native and synthetic cluster cores gives weighted rms deviations in atom positions of 0.20–0.38 Å. This study and an earlier investigation (Zhang, Y.; Holm, R. H. *J. Am. Chem. Soc.* **2003**, *125*, 3910–3920) provide a comprehensive account of the synthesis of structural analogues of the native P^N cluster and provide the basis for continuing investigation of the synthesis of weak-field Mo–Fe–S clusters related to nitrogenase. (Tp = tris(pyrazolyl)hydroborate(1–).)

Introduction

The concept that high-nuclearity metal-sulfur clusters may function as precursors to other clusters related in structure to the P-cluster (Fe_8S_9) and FeMo-cofactor cluster ($MoFe_7S_9$) of nitrogenase[1] has been supported by recent developments in this laboratory. The key precursors in our hands are edge-bridged double cubanes with the centrosymmetric cores $M_2Fe_6S_8 = M_2Fe_6(\mu_3\text{-}S)_6(\mu_4\text{-}S)_2$, exemplified by $[(Tp)_2Mo_2Fe_6S_8(PEt_3)_4]$ (**2**) in Figure 1. Clusters of this structure type having M = V,[2,3] Fe,[4,5] and Mo[6−10] have been synthesized recently. Certain of these molecules have been converted to clusters of the same nuclearity and a higher sulfur content in reactions with concomitant structural reorganization. The overall conversion in question is $[(Tp)_2M_2Fe_6S_8(PEt_3)_4] \rightarrow [(Tp)_2M_2Fe_6S_9(SH)_2]^{3-,4-}$ (M = V,[3,11] Mo[10,11]), in which the product core $M_2Fe_6S_9 = M_2Fe_6(\mu_2\text{-}S)_2(\mu_3\text{-}S)_6(\mu_6\text{-}S)$ has the topology of the P^N cluster of nitrogenase.[12,13]

* Corresponding author. E-mail: holm@chemistry.harvard.edu.

(1) Zhou, H.-C.; Su, W.; Achim, C.; Rao, P. V.; Holm, R. H. *Inorg. Chem.* **2002**, *41*, 3191−3201.
(2) Hauser, C.; Bill, E.; Holm, R. H. *Inorg. Chem.* **2002**, *41*, 1615−1624.
(3) Zuo, J.-L.; Zhou, H.-C.; Holm, R. H. *Inorg. Chem.* **2003**, 4624−4631.
(4) Goh, C.; Segal, B. M.; Huang, J.; Long, J. R.; Holm, R. H. *J. Am. Chem. Soc.* **1996**, *118*, 11844−11853.
(5) Zhou, H.-C.; Holm, R. H. *Inorg. Chem.* **2003**, *42*, 11−21.
(6) Demadis, K. D.; Campana, C. F.; Coucouvanis, D. *J. Am. Chem. Soc.* **1995**, *117*, 7832−7833.
(7) Osterloh, F.; Segal, B. M.; Achim, C.; Holm, R. H. *Inorg. Chem.* **2000**, *39*, 980−989.
(8) Osterloh, F.; Achim, C.; Holm, R. H. *Inorg. Chem.* **2001**, *40*, 224−232.
(9) Han, J.; Koutmos, M.; Al-Ahmad, S.; Coucouvanis, D. *Inorg. Chem.* **2001**, *40*, 5985−5999.
(10) Zhang, Y.; Holm, R. H. *J. Am. Chem. Soc.* **2003**, *125*, 3910−3920.
(11) Zhang, Y.; Zuo, J.-L.; Zhou, H.-C.; Holm, R. H. *J. Am. Chem. Soc.* **2002**, *124*, 14292−14293.
(12) Peters, J. W.; Stowell, M. H. B.; Soltis, S. M.; Finnegan, M. G.; Johnson, M. K.; Rees, D. C. *Biochemistry* **1997**, *36*, 1181−1187.
(13) Mayer, S. M.; Lawson, D. M.; Gormal, C. A.; Roe, S. M.; Smith, B. E. *J. Mol. Biol.* **1999**, *292*, 871−891.

10.1021/ic030259t CCC: $27.50
Published on Web 12/20/2003

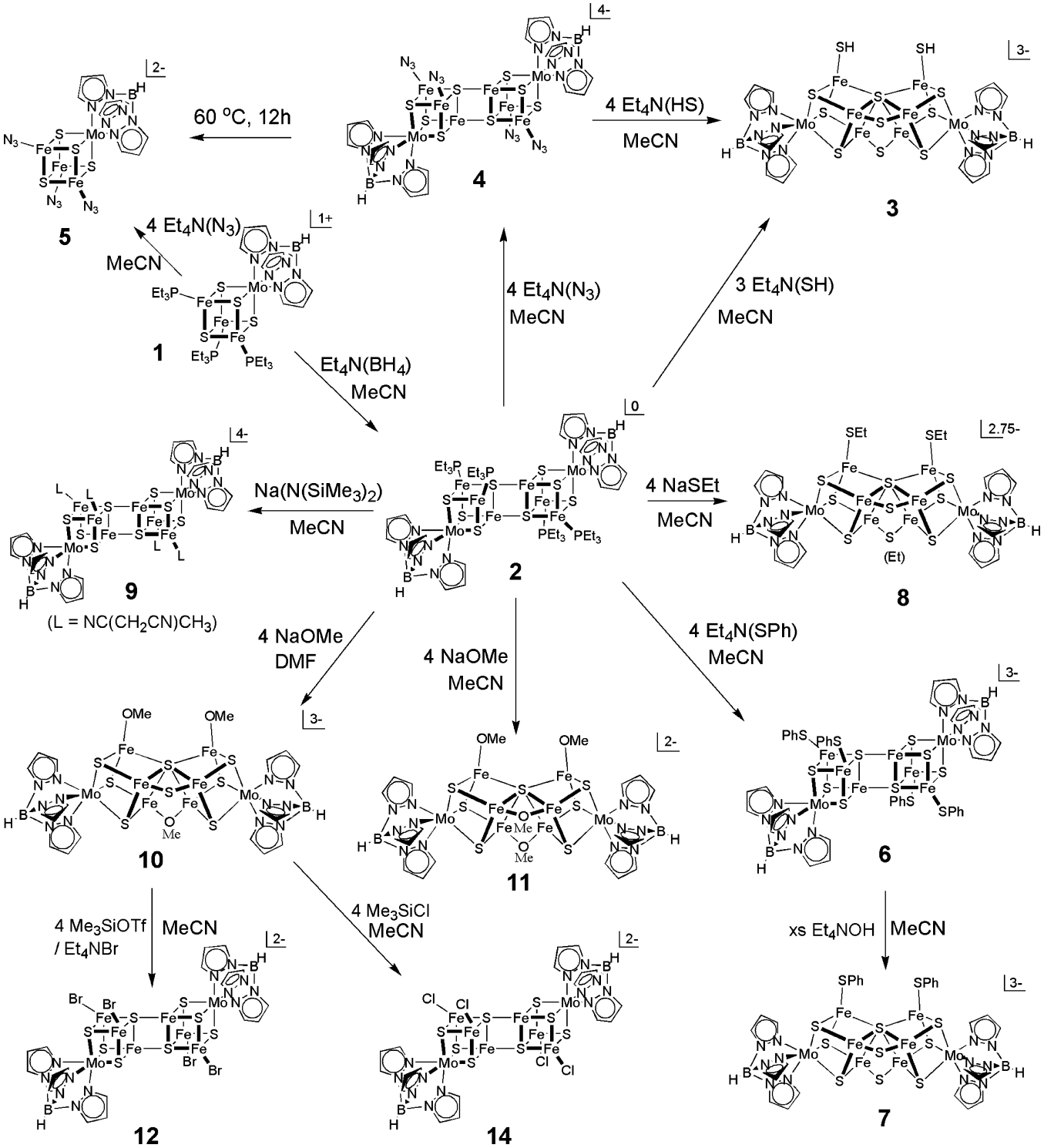

Figure 1. Synthetic scheme showing the transformation of edge-bridged double cubanes to other double cubanes (**2** → **4**, **6**, **9**) and to clusters with the P^N-cluster topology (**2** → **8**, **10**, **11**; **6** → **7**) and the conversion of the P^N cluster type to a double cubane (**10** → **12**, **14**).

Among the significant issues that accompany this structural conversion is the generality of its occurrence; i.e., what reagents other than hydrosulfide effect the conversion and what ligands and core compositions preserve the core topology. There is, further, the unfinished matter of determining the scope of stable double cubanes of possible eventual use in synthesis and the stability and reactivity of clusters with the P^N-cluster topology. The situation is compounded by the recent synthesis of an Fe_8S_7 species with this topology by a self-assembly process, presumably unrelated to our procedure, and the reported instability of the cluster in solution.[14] In this report, we provide observations which address in part these issues. This work continues our approach to the nitrogenase clusters by speculative synthetic chemistry, the philosophy and expectations of which are discussed elsewhere.[15]

(14) Ohki, Y.; Sunada, Y.; Honda, M.; Katsada, M.; Tatsumi, K. *J. Am. Chem. Soc.* **2003**, *125*, 4052−4053.

Table 1. Crystallographic Data for Compounds Containing Clusters **4**−**12** and **14**.[a]

	$(Et_4N)_4$[**4**]·2MeCN	$(Et_4N)_2$[**5**]	$(Et_4N)_3$[**6**]·MeCN	$(Et_4N)_3$[**7**]·5.5MeCN	$(Et_4N)_{2.75}$[**8**]·2.5MeCN
formula	$C_{54}H_{106}B_2Fe_6Mo_2N_{30}S_8$	$C_{25}H_{150}BFe_3MoN_{17}S_4$	$C_{68}H_{103}B_2Fe_6Mo_2N_{16}S_{12}$	$C_{65}H_{106.5}B_2Fe_6Mo_2N_{20.5}S_{11}$	$C_{48.5}H_{93.75}B_2Fe_6Mo_2N_{18}S_{11}$
fw	1980.77	991.36	2077.98	2076.47	1812.97
cryst syst	monoclinic	monoclinic	triclinic	monoclinic	triclinic
space group	$P2_1/c$	$P2_1/n$	$P\bar{1}$	$P2_1/n$	$P\bar{1}$
Z	2	4	1	4	2
a, Å	11.882(2)	10.6920(17)	12.333(3)	18.114(3)	14.938(4)
b, Å	20.771(4)	34.707(6)	13.935(3)	17.997(3)	17.094(4)
c, Å	17.159(3)	10.9322(18)	15.016(3)	27.898(4)	18.600(5)
α, deg	90	90	84.84(3)	90	79.331(5)
β, deg	99.818(4)	92.902(4)	72.41(3)	91.602(4)	78.884(5)
γ, deg	90	90	70.77(3)	90	64.905(5)
V, Å^3	4172.5(13)	4051.6(11)	2322.6(8)	9091(2)	4191.6(18)
GOF (F^2)	0.881	0.957	0.810	0.850	0.984
R_1[b], wR_2[c]	0.036, 0.059	0.045, 0.097	0.056, 0.122	0.058, 0.103	0.053, 0.151

	$(Et_4N)_4$[**9**]·3MeCN	$(Et_4N)_3$[**10**]·2DMF·C_6H_{14}	$(Et_4N)_2$[**11**]·MeCN	$(Et_4N)_2$[**12**]·2$C_4H_{10}O$	$(Et_4N)_2$[**14**]·4MeCN
formula	$C_{72}H_{119}B_2Fe_6Mo_2N_{27}S_8$	$C_{57}H_{131}B_2Fe_6Mo_2N_{17}O_5S_8$	$C_{40}H_{75}B_2Fe_6Mo_2N_{15}O_4S_7$	$C_{42}H_{80}B_2Br_4Fe_6Mo_2N_{14}O_2S_8$	$C_{42}H_{72}B_2Cl_4Fe_6Mo_2N_{18}S_8$
fw	2168.44	1939.64	1603.27	1937.80	1776.06
cryst syst	triclinic	monoclinic	monoclinic	orthorhombic	orthorhombic
space group	$P\bar{1}$	$C2/c$	$P2_1/n$	$Pbam$	$Ibam$
Z	1	8	4	2	4
a, Å	11.960(3)	28.932(8)	19.989(7)	15.359(3)	15.070(3)
b, Å	14.424(4)	20.688(6)	16.420(6)	19.810(4)	19.824(4)
c, Å	15.357(4)	31.443(9)	23.472(9)	11.806(2)	23.695(4)
α, deg	102.785(5)	90	90	90	90
β, deg	99.337(5)	116.398(6)	112.549(8)	90	90
γ, deg	97.038(5)	90	90	90	90
V, Å^3	2514.5(11)	16857(8)	7115(4)	3592(1)	7079(2)
GOF (F^2)	1.049	1.090	1.089	1.067	1.180
R_1[b], wR_2[c]	0.044, 0.124	0.079, 0.129	0.098, 0.262	0.042, 0.097	0.041, 0.118

[a] Collected using Mo Kα (λ = 0.710 73 Å) radiation at T = 193 K. [b] $R_1 = \sum||F_o| - |F_c||/\sum|F_o|$. [c] $wR_2 = \{\sum[w(F_o^2 - F_c^2)^2/\sum[w(F_o^2)^2]\}^{1/2}$.

Experimental Section

Preparation of Compounds. All procedures were carried out under a pure dinitrogen atmosphere using standard Schlenk and glovebox techniques. Ether and acetonitrile were passed through an Innovative Technologies solvent purification system. Methanol was distilled over magnesium, and toluene was distilled from sodium benzophenone ketyl. All solvents were further deoxygenated before use. Because of the small preparative scales employed, compounds were not analyzed. They were securely identified by X-ray structure determinations of all compounds and by ^{1}H NMR spectra of certain clusters. In some cases, not all proton resonances were detected (as found previously with related clusters) owing to paramagnetic signal broadening. When crystallized for structure determination, all but one compound were obtained as solvates (Table 1). In the preparations that follow, cluster reactant quantities and yields are calculated using unsolvated formula weights unless noted otherwise. Predicated on X-ray crystalline samples, solvates usually contribute ≲10% of the formula weight; the maximum is found with the compound containing cluster **10** (13%). While solvate contributions are not large, yields (all of which are based on the cluster reactant) should be considered as reproducible but approximate.

$(Et_4N)_4[(Tp)_2Mo_2Fe_6S_8(N_3)_4]$. To a suspension of 0.16 g (0.10 mmol) of $[(Tp)_2Mo_2Fe_6S_8(PEt_3)_4]$ in 15 mL of acetonitrile was added 0.069 g (0.40 mmol) of $(Et_4N)N_3$. The black solution which formed within 1 h was stirred for 3 h and filtered through Celite. Vapor diffusion of ether into the filtrate yielded the product as 0.15 g (75%) of black blocklike crystals. ^{1}H NMR (CD_3CN, anion): δ 5.40(4), 13.5 (br, 2), 16.1 (br, 2), 17.3 (br, 4), 19.4 (4), 26.1 (2).

$(Et_4N)_2[(Tp)MoFe_3S_4(N_3)_3]$. A solution of 0.245 g (0.20 mmol) of $[(Tp)MoFe_3S_4(PEt_3)_3](BPh_4)$[10] in 30 mL of acetonitrile was added to a solution of 0.112 g (0.65 mmol) of $(Et_4N)N_3$ in 10 mL of acetonitrile. The black solution was allowed to stand for 16 h and was filtered through Celite. Diffusion of ether into the filtrate caused separation of the product as 0.142 g (72%) of black crystals. ^{1}H NMR (CD_3CN, anion): δ 5.00 (3),18.0 (3).

$(Et_4N)_3[(Tp)_2Mo_2Fe_6S_9(SH)_2]$. A solution of 0.020 g (0.010 mmol) of $(Et_4N)_4[(Tp)_2Mo_2Fe_6S_8(N_3)_4]$ in 5 mL of acetonitrile was added to a solution of 0.007 g (0.04 mmol) of $Et_4N(HS)$ in 5 mL of acetonitrile. The black solution was allowed to stand for 16 h and filtered through Celite. Vapor diffusion of ether into the filtrate afforded the product as 0.013 g (62%) of black crystals. The identity of this compound was confirmed by its cell parameters and an ^{1}H NMR spectrum identical to that of an authentic sample.[10]

$(Et_4N)_3[(Tp)_2Mo_2Fe_6S_8(SPh)_4]$. To a suspension of 0.16 g (0.10 mmol) of $[(Tp)_2Mo_2Fe_6S_8(PEt_3)_4]$ in 15 mL of acetonitrile was added 0.096 g (0.40 mmol) of $(Et_4N)(SPh)$. The dark green solution which formed was stirred for 6 h and filtered through Celite. Vapor diffusion of ether into the filtrate afforded the product as 0.15 g (73%) of dark green platelike crystals. ^{1}H NMR (CD_3CN, anion): δ −13.9 (8, *o*-H), −13.2 (4, *p*-H), 5.0 (4), 10.5 (br, 4), 16.7 (4), 19.1 (8, *m*-H), 22.4 (2).

$(Et_4N)_3[(Tp)_2Mo_2Fe_6S_9(SPh)_2]$. A solution of 0.052 g (0.025 mmol) of $(Et_4N)_3[(Tp)_2Mo_2Fe_6S_8(SPh)_4]$ in 8 mL of acetonitrile was treated with a solution of 0.036 g (0.25 mmol) of Et_4NOH in 2 mL of acetonitrile. The dark brown solution was stirred for 12 h and filtered through Celite. Vapor diffusion of ether into the filtrate resulted in separation of the product as 0.017 g (36%) of black crystalline product after washing with ether. ^{1}H NMR (CD_3CN, anion): δ −16.0 (4, *o*-H), 13.8 (2, *p*-H), 4.70 (4), 8.30 (2-H), 13.2 (4), 13.3 (2), 17.3 (4, *m*-H), 18.2 (4), 21.9 (br, 2).

$(Et_4N)_{2.75}[(Tp)_2Mo_2Fe_6S_{8.75}(SEt)_{2.25}]$. A mixture of 0.064 g (0.40 mmol) of Et_4NCl and 0.033 g (0.40 mmol) of NaSEt in 15 mL of acetonitrile was stirred for 2 h. The suspension was filtered into a solution of 0.16 g (0.10 mmol) of $[(Tp)_2Mo_2Fe_6S_8(PEt_3)_4]$ in 15

(15) Lee, S. C.; Holm, R. H. *Proc. Natl. Acad. Sci. U.S.A.* **2003**, *100*, 3595−3600, 12522−12527.

mL of acetonitrile. The black solution that formed within 1 h was stirred for 6 h and filtered through Celite. Vapor diffusion of ether into the filtrate afforded the product as 0.13 g (70%) of a black crystalline product. This material was identified as a mixture of two clusters by an X-ray structure determination.

$(Et_4N)_4[(Tp)_2Mo_2Fe_6S_8(NC(Me)CH_2CN))_4]$. $NaN(SiMe_3)_2$ (0.073 g, 0.40 mmol) was added to a suspension of 0.16 g (0.10 mmol) of $[(Tp)_2Mo_2Fe_6S_8(PEt_3)_4]$ in 15 mL of acetonitrile. The dark green solution that formed within 1 h was stirred for 6 h and filtered through Celite. Vapor diffusion of ether into the filtrate gave the product as 0.186 g (88%) of dark green blocklike crystals. $E_{1/2} = -0.98$, -1.52 V (acetonitrile).

$(Et_4N)_2[(Tp)_2Mo_2Fe_6S_8(OMe)_3]$. A mixture of 0.064 g (0.40 mmol) of Et_4NCl and 0.021 g (0.40 mmol) of NaOMe in 10 mL of DMF was stirred for 1 h and filtered into a suspension of 0.16 g (0.10 mmol) of $[(Tp)_2Mo_2Fe_6S_8(PEt_3)_4]$ in 15 mL of DMF. The suspension became homogeneous and formed a dark green solution within 1 h. The solution was stirred for 6 h and filtered through Celite. Ether was introduced into the filtrate by vapor diffusion, causing separation of the product as 0.132 g (74%) of dark green blocklike crystals. The compound analyzed satisfactorily as the bis(DMF) solvate; the yield is based on this formulation. Anal. Calcd for $C_{51}H_{117}B_2Fe_6Mo_2N_{17}O_5S_8$: C, 33.02; H, 6.31; N, 12.84; Fe, 18.07; Mo, 10.35, S, 13.81. Found: C, 33.19; H, 5.90; N, 12,64; Fe, 17.94; Mo, 10.29; S, 13.60.

$(Et_4N)_2[(Tp)_2Mo_2Fe_6S_7(OMe)_4]$. The previous preparation was followed but with use of 15 mL of acetonitrile as the reaction solvent. Ether diffusion produced a mixture of dark green platelike crystals and a black noncrystalline solid. The crystals were mechanically separated. The identity of the crystalline product was established by an X-ray structure determination.

$(Et_4N)_2[(Tp)_2Mo_2Fe_6S_8Br_4]$. A solution of 0.036 g (0.020 mmol) of $(Et_4N)_2[(Tp)_2Mo_2Fe_6S_8(OMe)_3]$ in 10 mL of acetonitrile was treated with 0.015 g (0.080 mmol) of $Me_3SiOSO_2CF_3$. After several minutes, 0.017 g (0.080 mmol) of Et_4NBr was added. The dark green solution was stirred for 6 h and filtered through Celite. Vapor diffusion of ether into the filtrate caused the product to separate as 0.026 g (77%) of dark green crystals. ^{1}H NMR (CD_3CN): δ 4.2 (br, 1), 7.70 (2), 9.80 (2), 21.7 (br, 1), 35.3 (br, 1). $E_{1/2} = -0.82$ V acetonitrile).

$(Et_4N)_2[(Tp)_2Mo_2Fe_6S_8Cl_4]$. A solution of 0.0090 g (0.080 mmol) of Me_3SiCl in 2 mL of acetonitrile was added to a solution of 0.038 g (0.020 mmol) of $[(Tp)_2Mo_2Fe_6S_8(PEt_3)_4]$ in 8 mL of acetonitrile. The black solution was stirred for 1 h and filtered through Celite. Vapor diffusion of ether into the filtrate resulted in the formation of black blocklike crystals and platelike crystals in about equal amounts. The former was separated by hand and demonstrated to be the title compound by an X-ray structure determination. ^{1}H NMR (CD_3CN): δ 7.40 (2), 10.2 (2), 22.8 (br, 1), 35.3 (br, 1). $E_{1/2} = -0.87$ V (acetonitrile). The platelike crystals were shown to be $(Et_4N)_3[(Tp)_2Mo_2Fe_6S_8Cl_4]$ by a fast X-ray data set (details not reported).

In the sections that follow, clusters are designated numerically as **1**−**14** according to Chart 1.

X-ray Structure Determinations. The structures of the 10 compounds in Table 1 were determined. Diffraction-quality crystals were obtained by vapor diffusion of ether into acetonitrile solutions or, in the case of $(Et_4N)_3$[**10**], a solution in DMF containing hexane. Crystals were mounted in Infineum oil on a fiber on a goniometer head which was placed in the dinitrogen cold stream on a Siemens (Bruker) SMART CCD-based diffractometer at 193 K. Cell parameters were retrieved using SMART software and refined using SAINT on all observed reflections. Data were collected using 0.3° intervals in φ and ω for 30 s/frame such that a hemisphere of data was collected. A total of 1271 frames were collected with a maximum resolution of 0.75 Å. The first 50 frames were recollected at the end of the data collection to monitor intensity decay; none was found. The highly redundant data sets were reduced with use of SAINT and corrected for Lorentz and polarization effects. Absorption corrections were applied with SADABS supplied by Bruker. Structures were solved by direct methods using SHELX-97.The position of metal atoms and their first coordination sphere atoms were located from *E* maps. Other non-hydrogen atoms were found in alternating difference Fourier syntheses and least-squares refinement cycles and, during the final cycles, were refined anisotropically. Hydrogen atoms were placed in calculated positions and refined as riding atoms with a uniform value of U_{iso}. Crystallographic parameters are collected in Table 1.[16]

Chart 1. Designation of Clusters[a]

$[(Tp)MoFe_3S_4(PEt_3)_3]^{1+}$	**1**[10]
$[(Tp)_2Mo_2Fe_6S_8(PEt_3)_4]$	**2**[10]
$[(Tp)_2Mo_2Fe_6S_9(SH)_2]^{3-}$	**3**[10,11]
$[(Tp)_2Mo_2Fe_6S_8(N_3)_4]^{4-}$	**4**
$[(Tp)MoFe_3S_4(N_3)_3]^{2-}$	**5**
$[(Tp)_2Mo_2Fe_6S_8(SPh)_4]^{3-}$	**6**
$[(Tp)_2Mo_2Fe_6S_9(SPh)_2]^{3-}$	**7**
$[(Tp)_2Mo_2Fe_6S_{8.75}(SEt)_{2.25}]^{2.75-}$	**8**
$[(Tp)_2Mo_2Fe_6S_8(N_2C_4H_5)_4]^{4-}$	**9**
$[(Tp)_2Mo_2Fe_6S_8(OMe)_3]^{3-}$	**10**
$[(Tp)_2Mo_2Fe_6S_7(OMe)_4]^{2-}$	**11**
$[(Tp)_2Mo_2Fe_6S_8Br_4]^{2-}$	**12**
$[(Tp)_2Mo_2Fe_6S_8Cl_4]^{4-}$	**13**[10]
$[(Tp)_2Mo_2Fe_6S_8Cl_4]^{2-}$	**14**

[a] Tp = tris(pyrazolyl)hydroborate(1−).

Other Physical Measurements. All measurements were performed under anaerobic conditions. ^{1}H NMR spectra were collected using a Varian AM-300 spectrometer. Cyclic voltammograms were recorded with a Princeton Applied Research model 263 potentiostat/galvanostat using a Pt working electrode and 0.1 M $(Bu_4N)(PF_6)$ supporting electrolyte. Potentials are referenced to the saturated calomel electrode (SCE).

Results and Discussion

Shown in Figure 1 is a synthetic scheme summarizing three types of cluster transformations: (i) terminal ligand substitution of edge-bridged phosphine double cubane **2**,[10] the principal cluster reactant in this work, to other cubanes with the same core structure and (ii) to clusters with the P^N-cluster topology, and (iii) conversion of the P^N-cluster type to a double cubane. Each of these reaction types is considered in turn. The protocol is straightforward: ambient temperature reaction between cluster and ligand, filtration of the reaction mixture, and vapor diffusion of ether into the filtrate, all steps being under anaerobic conditions. X-ray structures are presented as the definitive means of product identification. Analytical, electrochemical, and spectroscopic data, alone or in combination, are not capable of structure proof. All clusters contain trigonally distorted octahedral MoN_3S_3 sites

(16) See paragraph at the end of this article for Supporting Information available.

Table 2. Selected Bond Distances (Å) and Angles (deg) of Edge-Bridged Double Cubanes

	4	6	9	12	14
			Cubane[a]		
Mo−Fe	2.72(3)	2.71(2)	2.73(3)	2.70(1)	2.700(4)
Fe−Fe	2.60(3)	2.691(9)	2.61(3)	2.69(4)	2.70(3)
Mo−S	2.37(1)	2.371(7)	2.380(6)	2.364(9)	2.363(8)
Fe−S	2.283(6)	2.256(9)	2.28(1)	2.25(1)	2.25(2)
Fe−S_{br}[b]	2.384(1)	2.365(3)	2.39(2)	2.332(6)	2.340(2)
Fe−L	2.02(1)	2.28(1)	2.010(8)[e]	2.368(1)	2.225(2)
			Bridge Rhomb		
Fe−Fe	2.868(9)	2.596(2)	2.72(1)	2.595(2)	2.603(2)
Fe−S[c]	2.422(8)	2.394(2)	2.44(1)	2.318(2)	2.312(2)
Fe−S[d]	2.284(8)	2.243(2)	2.25(1)	2.240(2)	2.226(2)
Fe−S−Fe	75.04(3)	67.99(7)	70.55(4)	69.40(5)	69.96(6)
S−Fe−S	104.96(3)	112.01(7)	109.15(4)	110.60(5)	110.04(6)

[a] Mean values. [b] Fe−μ_4-S. [c] Intracubane. [d] Intercubane. [e] Ordered ligand:

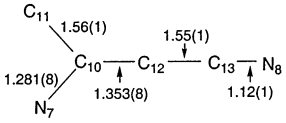

C_{11}-C_{10}-C_{12} 112.5(7)°
N_7-C_{10}-C_{12} 134.1(8)°
C_{10}-C_{12}-C_{13} 113.9(8)°
C_{12}-C_{13}-N_8 175(1)°

Table 3. Mean Values of Selected Bond Distances (Å) and Angles (deg) in P^N-type Clusters

	7	10	11	P^N cluster[e]
Mo−N	2.24(1)	2.25(1)	2.247(5)	
Mo−S	2.37(1)	2.38(1)	2.38(1)	
Fe−OMe		1.89(1)	1.898(6)	
Fe−μ_2-S	2.226(3)	2.249(2)		2.41
Fe−μ_2-O		2.010(1)	1.97(2)	
Fe−μ_3-S	2.257(6)	2.27(1)	2.27(1)	2.30
Fe−μ_6-S	2.38(1)	2.42(2)	2.46(3)	2.45
Fe−Fe[a]	2.692(4)	2.83(3)	2.878(4)[c] 2.761(4)[d]	2.93
Fe−Fe′[b]	2.73(4)	2.64(2)	2.60(2)	2.54
Fe−μ_2-S−Fe′	74.40(7)	77.6(1)		74
Fe−μ_2-O−Fe′		90.2(5)	91(2)	
Fe−μ_6-S−Fe′[f]	144.0(1)	149.4(2)	157.4(2)	158

[a] Intercubane. [b] Intracubane. [c] Fe2−Fe5. [d] Fe3−Fe6. [e] Values quoted in ref 13. [f] Maximum value (edge angle). Other clusters: **3**, 141.0(1)°; **8**, 151.8(1)°.

and distorted tetrahedral FeS_3X sites. Double cubanes and P^N-type clusters (excluding **10**) have actual or idealized C_{2h} and C_{2v} core structures, respectively. Because of the large body of metric data[16] and extensive descriptions of single cubane, edge-bridged double cubane, and P^N-cluster type structures provided elsewhere,[3,7−10,17,18] structural information is confined to Figures 2, 3, 5, and 6 and the mean bond lengths in Tables 2 and 3.

Terminal Ligand Substitution of Edge-Bridged Double Cubanes. Cluster **2** undergoes facile ligand substitution with 4 equiv of azide to afford **4** (75%), isolated in the indicated yield as the Et_4N^+ salt. This process is an example of generalized substitution reaction 1, which has been reported for M = Mo, L = Cl^- [10] and M = V, L = Cl^-, PhS^-.[2] These reactions proceed in good yield with retention of the

$$[(Tp)_2M_2Fe_6S_8(PEt_3)_4] + 4L^- \rightarrow [(Tp)_2M_2Fe_6S_8L_4]^{4-} + 4PEt_3 \quad (1)$$

ferrous $[M_2Fe_6S_8]^{2+}$ core, unlike reactions with certain other nucleophiles (vide infra). The formation of thiolate cluster **6** likely takes place according to reaction 1 except that the product contains the one-electron oxidized core $[Mo_2Fe_6S_8]^{3+}$. This cluster is one electron more reduced than $[(Tp)_2V_2Fe_6S_8(SPh)_4]^{4-}$,[2] with which it is isostructural. Cluster **6** shows two quasi-reversible oxidations at −1.01 and −0.47 V, implying substantial oxidative instability of the species $[(Tp)_2Mo_2Fe_6S_8(SPh)_4]^{4-}$, the putative product of reaction 1. The oxidant leading to **6** has not been identified. The more electronegative ligands azide and chloride sustain the $[Mo_2Fe_6S_8]^{2+}$ oxidation level. The structures of **4** and **6** are set out in Figures 2 and 3, respectively. While not all Tp protons in **6** could be located, presumably because of paramagnetic broadening, the ^{1}H NMR spectrum in Figure 4 is consistent with a C_i structure containing two types of pyrazolyl rings in a 2:1 ratio.

Nitrogenous ligand binding is of interest as a potential means of eventually introducing an interstitial nitride atom in clusters. An interstitial atom, probably oxygen or nitrogen, is present in the FeMo-cofactor cluster of nitrogenase.[19] In a further experiment with a potential nitrogen ligand, a solution of cluster **2** in THF was treated with 4 equiv of $NaN(SiMe_3)_2$. However, no crystalline product was obtained. The same system in acetonitrile resulted in an immediate reaction, leading to the isolation of dark green $(Et_4N)_4$[**9**] (88%). A structure determination revealed that the ligands at the iron sites are not the silylimide but rather the condensation product of monodeprotonated acetonitrile, formed upon reaction with solvent and the highly basic imide, and acetonitrile itself. This species has been previously observed as the cathodic breakdown product of acetonitrile in the absence of water.[20] Further, it has been isolated as a lithium salt from the reaction of Li[$NBu^t(SiMe_3)$] and acetonitrile and its X-ray structure has been determined.[21] The ion has two tautomeric forms, $[MeC(=N)CH_2CN]^-$ and $[MeC(NH)=CHCN]^-$. The structure of the lithium salt has been interpreted in terms of the latter form. Centrosymmetric cluster **9** in the crystal shows one ordered and one disordered ligand (Figure 2). Parameters of the ordered ligand (Table 3) accord satisfactorily with monodeprotonated 2-iminobutyrylnitrile. Note that the terminal Fe−L bond distances of **4** and **9** are indistinguishable. The azide single cubane **5** (Figure 2) can be prepared by heating an acetonitrile solution of **4** (Figure 1) or by the reaction of $[(Tp)MoFe_3S_4(PEt_3)_3]^+$ with 3 equiv of azide in acetonitrile. The mean Fe−N bond distance in **5** (1.966(9) Å) is marginally shorter than that in **4** (2.02(1) Å), probably because the $[MoFe_3S_4]^{2+}$ core is one-electron more oxidized (increased ferric character) than the cubane units in **5**. Last, the role of solvent is further evident in the reaction of $[Fe_4S_4(PCy_3)_4](BPh_4)$[4] and $NaN(SiMe_3)_2$ in THF, which affords a silylimido-ligated product,

(17) Demadis, K. D.; Coucouvanis, D. *Inorg. Chem.* **1995**, *34*, 436−448.
(18) Malinak, S. M.; Coucouvanis, D. *Prog. Inorg. Chem.* **2001**, *49*, 599−662.
(19) Einsle, O.; Tezcan, F. A.; Andrade, S.; Schmid, B.; Yoshida, M.; Howard, J. B.; Rees, D. C. *Science* **2002**, *297*, 1696−1700.
(20) Foley, J. K.; Korzeniewski, C.; Pons, S. *Can. J. Chem.* **1988**, *66*, 201−206.
(21) Avent, A. G.; Frankland, A. D.; Hitchcock, P. B.; Lappert, M. F. *J. Chem. Soc., Chem. Commun.* **1996**, 2433−2434.

$[(Tp)_2Mo_2Fe_6S_8(N_3)_4]^{4-}$

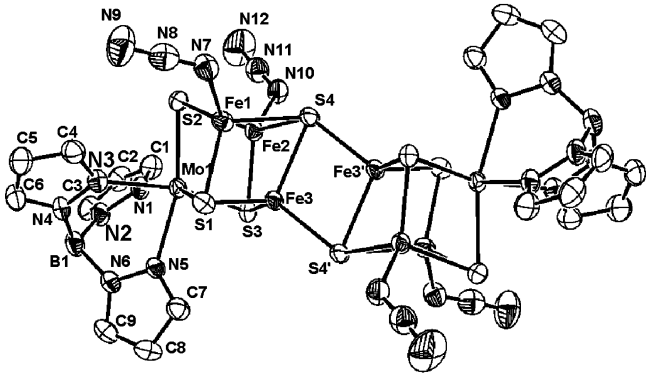

$[(Tp)MoFe_3S_4(N_3)_3]^{2-}$

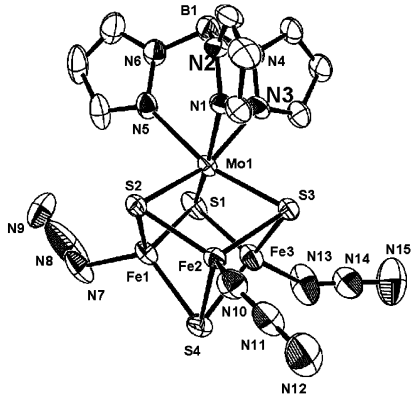

$[(Tp)_2Mo_2Fe_6S_8(NC(CH_2CN)CH_3)_4]^{4-}$

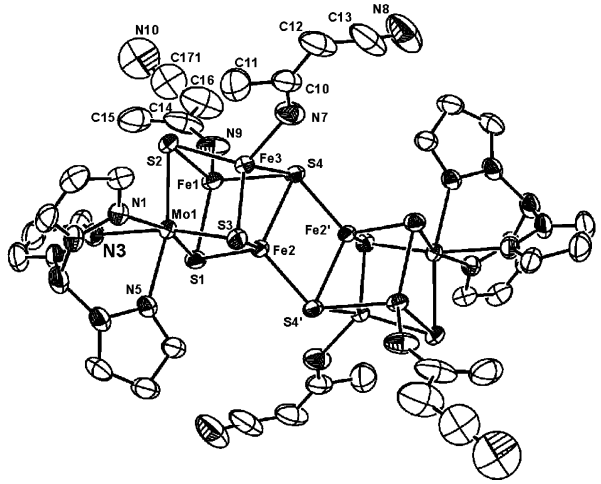

Figure 2. Structures of edge-bridged double cubane **4** (upper), single cubane **5** (middle), and edge-bridged double cubane **9** (lower). Cluster **4** has crystallographically imposed centrosymmetry. In this and succeeding figures, 50% probability ellipsoids and partial atom numbering schemes are shown. In **9**, the ligand containing N9 is shown in one of two disordered positions of equal occupancy. In **4** and **6**, Fe−N−N angles are in the range 124.5(4)−136.3(5)° and the azide ligands are essentially linear.

centrosymmetric $[Fe_8S_8(PCy_3)_4(N(SiMe_3)_2]$.[22] This cluster is isoelectronic and isostructural with $[Fe_8S_8(PPr^i_3)_4(SSiPh_3)_2]$.[5]

$[(Tp)_2Mo_2Fe_6S_8(SPh)_4]^{3-}$

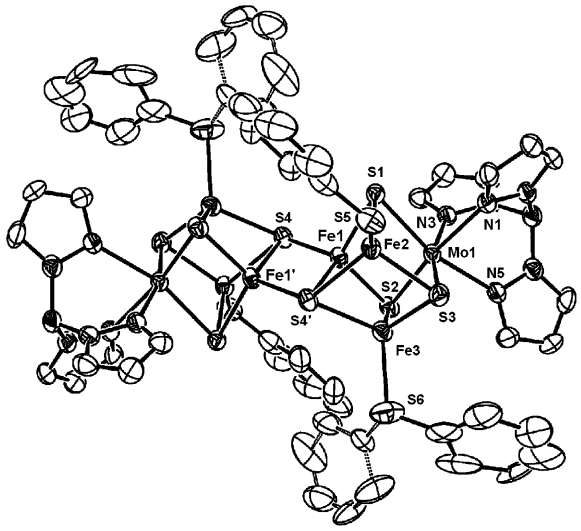

$[(Tp)_2Mo_2Fe_6S_9(SPh)_2]^{3-}$

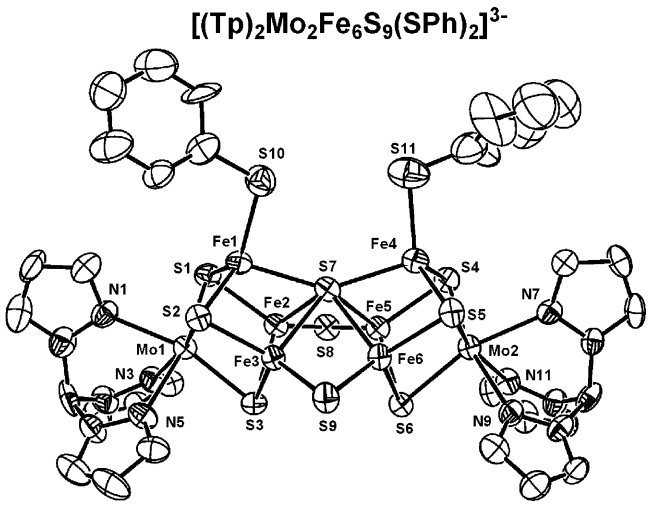

Figure 3. Structures of edge-bridged double cubane **6** with crystallographically imposed centrosymmetry (upper) and P^N-type cluster **7** (lower). One phenyl ring of **6** is disordered over two positions with equal populations.

P^N-Type Clusters from Edge-Bridged Double Cubanes. Conversions of this type observed in this and previous work, by which an edge-bridged double cubane is transformed to a P^N-type cluster, may be summarized by the formal reaction types 2−5. The source of sulfide is either Li_2S or the cluster reactant; all reactions were performed in acetonitrile at ambient temperature. Reaction 2 is a redox process. In reactions 3−5, the core units do not change oxidation state. Each reaction type is considered in turn.

2 → 3, 4 → 3, 2 → 8:

$$[Mo_2Fe_6S_8]^{2+} + S^{2-} \rightarrow [Mo_2Fe_6S_9]^{+} + e^{-} \quad (2)$$

6 → 7:

$$[Mo_2Fe_6S_8]^{3+} + S^{2-} \rightarrow [Mo_2Fe_6S_9]^{+} \quad (3)$$

2 → 10:

$$[Mo_2Fe_6S_8]^{2+} \rightarrow *[Mo_2Fe_6S_8]^{2+} \quad (4)$$

2 → 11:

$$[Mo_2Fe_6S_8]^{2+} \rightarrow [Mo_2Fe_6S_7]^{4+} + S^{2-} \quad (5)$$

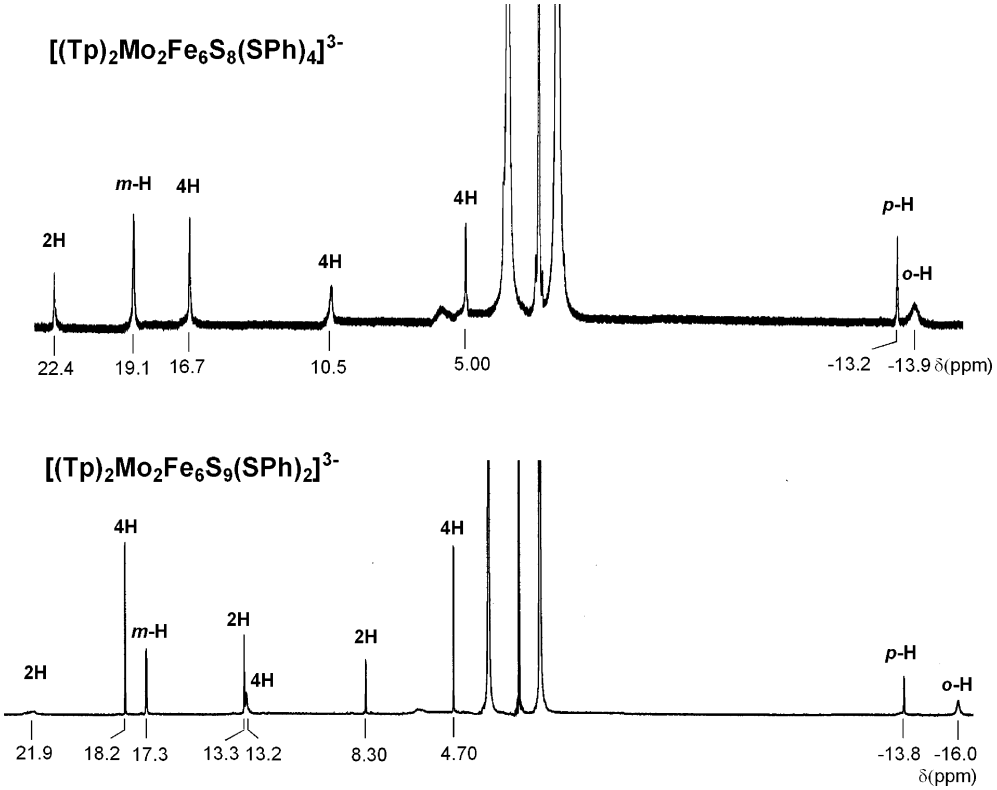

Figure 4. ^{1}H NMR spectra of clusters **6** (upper) and **7** (lower) in CD_3CN solutions at 298 K. Signal assignments are indicated; 2H and 4H refer to relative intensities of Tp signals.

(a) Reaction 2. This type subsumes three cluster conversions and requires an electron acceptor. The transformation **2** → **3** is the original route to P^N-type clusters and led to isolation of the product cluster in ca. 80% yield.[10,11] Reaction 6 (L = PEt_3, $z = 0$) was proposed with one-half equivalent of dihydrogen being the reduced product. The conversion **4** → **3** affords the product, identified by ^{1}H NMR,[10] in good

$$[(Tp)_2Mo_2Fe_6S_8L_4]^{z-} + 3HS^- \rightarrow [(Tp)_2Mo_2Fe_6S_9(SH)_2]^{3-} + 4L^{z-} + 1/2H_2 \quad (6)$$

yield (62%) and is describable in terms of reaction 6 (L = N_3^-, $z = 4$). Reaction of **2** with 4 equiv of NaSEt resulted in a black product **8** containing two clusters as Et_4N^+ salts whose crystal structure refined satisfactorily as an ca. 3:1 mixture (Figure 5). The majority product is $[(Tp)_2Mo_2Fe_6S_9(SEt)_2]^{3-}$, analogous to **7**. The minority product appears to be $[(Tp)_2Mo_2Fe_6S_8(\mu_2\text{-SEt})(SEt)_2]^{2-}$. Because this reaction system gave mixed products, it was not further investigated.

(b) Reaction 3. Treatment of **6** with 10 equiv of Et_4NOH results in the formation of **7** (36%). Hydroxide presumably causes partial cluster degradation with liberation of sulfide, some or all of which is incorporated in the product which is formed in moderate yield (36%). An X-ray structure demonstrates that **7** has the P^N cluster topology (Figure 3). This cluster is readily distinguishable from the precursor cluster by its ^{1}H NMR spectrum (Figure 4). All resonances are observed and are consistent with a C_{2v} structure. The positive isotropic shifts of *o*-H and *p*-H and the negative isotropic shift of *m*-H are indicative of dominant contact interactions, a consistent properties of all Fe−S and $MoFe_3S_4$ clusters investigated to date.

The essential features of **7** are a μ_6-S atom, bond lengths that decrease in the usual order Fe-μ_2S < Fe-μ_3S < Fe-μ_6S, a markedly obtuse Fe−μ_6S−Fe angle of 144.0(1)°, a mean terminal Fe−S distance of 2.28(1) Å, and trigonally distorted octahedral MoN_3S_3 coordination units. Certain numerical values are collected in Table 3. The cluster is isostructural with **3**, the first cluster prepared with P^N topology, for which a detailed structural description is given elsewhere.[10] The mean iron oxidation state from ^{57}Fe Mössbauer isomer shift data is most likely $Fe^{2.17+}$.[10] This reaction system was originally examined to determine whether oxide could be incorporated in the core structure of either an edge-bridged double cubane reactant or a product cluster. However, no oxygen-containing clusters could be identified.

(c) Reactions 4 and 5. The products of these reactions were established by the X-ray structure determinations in Figure 5. In the conversion **2** → **10**, the Mo−Fe−S portions of reactant and product have same composition but different structures, as indicated by the asterisk in reaction 4. Treatment of **2** with 4 equiv of methoxide in DMF afforded the dark green product **10** (74%). Two equivalents of methoxide are deployed as Fe−OMe terminal ligands and one as μ_2-OMe in the P^N-type structure of **10**. This reaction system effecting the conversion **2** → **11** was identical to reaction 4 except that it was performed in acetonitrile. Dark green crystals were separated from an accompanying black solid

(22) Zhang, Y.; Holm, R. H. Unpublished results.

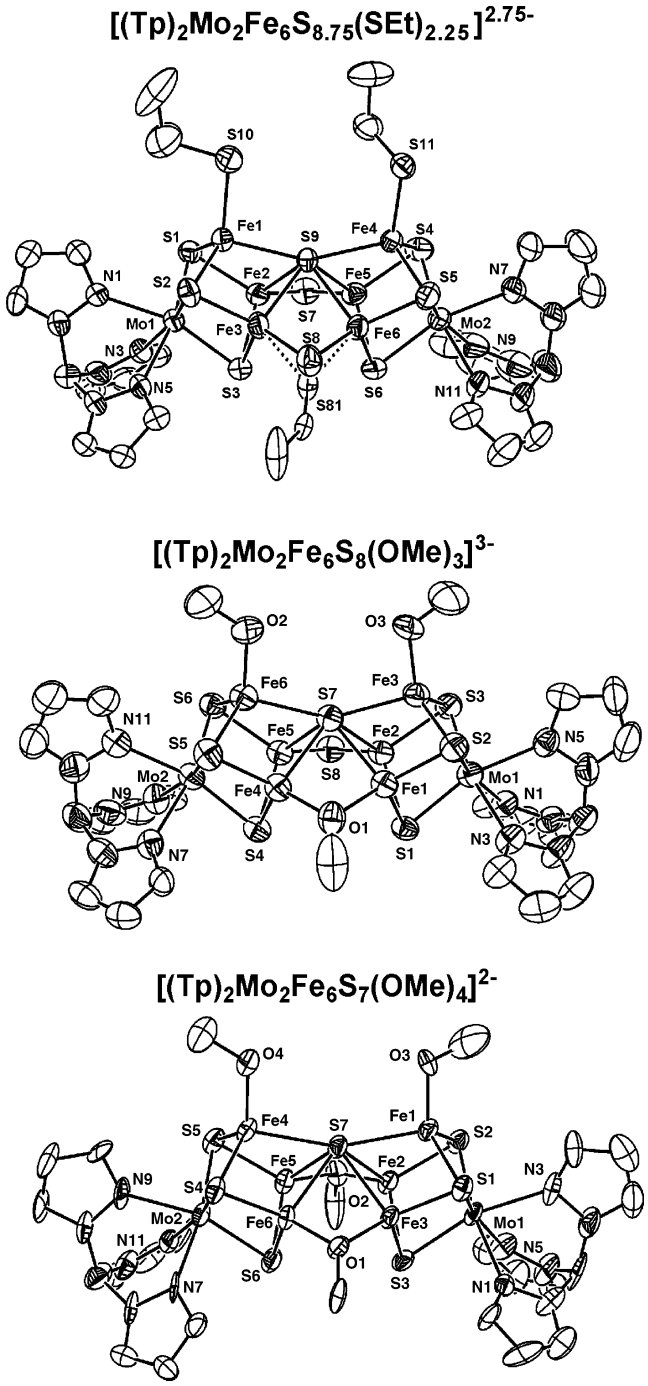

Figure 5. Structures of P^N-type clusters **8** (upper, a mixture of two clusters; see text), **10** (middle), and **11** (lower).

and were shown to contain four methoxide ligands by an X-ray structure determination (Figure 5). Two are in terminal positions as in **10**, and the other two are bridging. Hence, this conversion results in a cluster with the same idealized symmetry as **3** and **7**. The principal structural consequences of introducing one or two bridging methoxide groups in place of bridging thiolates are evident from Table 3. Bridge angles increase by 16−17°, intercubane Fe−Fe and Fe−μ_6S bond distances increase, and Fe−μ_6S−Fe angles become more obtuse, reaching the maximum value of 157.4(2)° in **11**. The Fe−μ_3S distances are essentially unaffected. The observed trends appear to correlate with the general tendency of oxygen to assume large bond angles than sulfur at parity of terminal ligands, a behavior that has been documented in binuclear iron complexes.[23]

Edge-Bridged Double Cubane from P^N-Type Cluster. Six conversions of an $Mo_2Fe_6S_8$ edge-bridged double cubane to a P^N-type cluster have now been executed (Figure 1). In addition, the corresponding conversion of a $V_2Fe_6S_8$ double cubane has been accomplished.[3,11] We became interested in the possibility of the reverse transformation. Cluster **10** lends itself to this inquiry because removal of its methoxide bridge recovers the core composition of an edge-bridged double cubane. Reaction of **10** with 4 equiv of Me_3SiOTf/Et_4NBr or Me_3SiCl in acetonitrile does indeed generate that the double cubane structure in the form of dianions **12** and **14**, respectively. We conjecture that reaction 7 ($L^- = Cl^-, Br^-$) occurs, which is expected to afford a tetraanion such as the previously reported chloride cluster **13**.[10] However, the products isolated were the two-electron oxidized dianions,

$$[(Tp)_2Mo_2Fe_6S_8(OMe)_3]^{3-} + 3Me_3SiL + L^- \rightarrow [(Tp)_2Mo_2Fe_6S_8L_4]^{4-} + 3Me_3SiOMe \quad (7)$$

which were identified crystallographically (Table 2). The reactions are reproducible; the oxidant has not been identified. The tetraanions are apparently oxidized in the ca. 1 day period required to grow crystals by vapor diffusion of ether into the acetonitrile reaction filtrate.

The likelihood of adventitious oxidation follows from electrochemical observations. Dianions **12** and **14** exhibit quasireversible 2−/3− reductions at $E_{1/2} = -0.82$ and −0.87 V, respectively. However, no well-defined 3−/4− steps were observed, a behavior also found for **4**. Addition of excess halide (to repress possible ligand dissociation) resulted in double cubane cleavage and the appearance of the redox step $[(Tp)MoFe_3S_4L_3]^{-/2-}$ at −0.56 V ($L = Cl^-$)[24] and −0.53 V ($L = Br^-$). In contrast, cluster **9** showed two quasireversible steps at −0.98 V (2−/3−) and −1.52 V (3−/4−). Accordingly, we estimate that the 3−/4− potentials of **12** and **14** are near −1.4 V, rendering the 4− clusters highly sensitive to oxidation.

The structures of chloride-substituted tetraanion **13**[10] and dianion **14** are compared in Figure 6. Clusters **12**−**14** have imposed centrosymmetry and both dianions also have a crystallographic mirror place, resulting in molecular C_{2h} symmetry. The most conspicuous feature upon passing from the $[Mo_2Fe_6S_8]^{2+}$ to the $[Mo_2Fe_6S_8]^{4+}$ oxidation state is the shortening of all Fe−S bonds upon oxidation, with the effect on the bridging rhomb being most noticeable. Further, the Fe−Cl distance is 0.10 Å shorter in the dianion, consistent with increased ferric character in the core. These effects are well documented with Fe_4S_4 clusters.[25,26] The Fe−Cl distance

(23) Mukherjee, R. N.; Stack, T. D. P.; Holm, R. H. *J. Am. Chem. Soc.* **1988**, *110*, 1850−1861.
(24) Fomitchev, D. V.; McLauchlan, C. C.; Holm, R. H. *Inorg. Chem.* **2002**, *41*, 958−966.
(25) Venkateswara Rao, P.; Holm, R. H. *Chem. Rev.* **2004**, *104*, 0000.
(26) Segal, B. M.; Hoveyda, H. R.; Holm, R. H. *Inorg. Chem.* **1998**, *37*, 3440−3443.

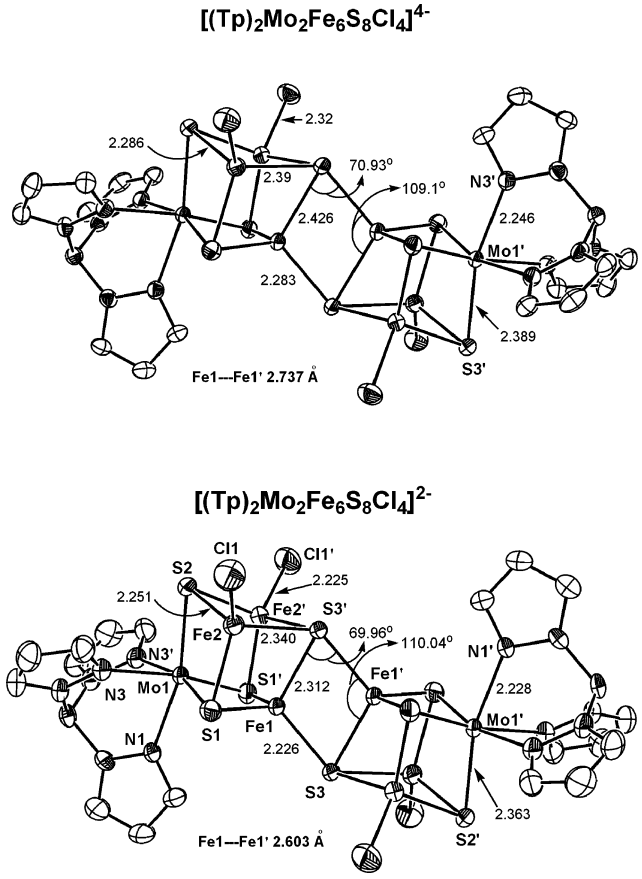

Figure 6. Structures of the edge-bridged double cubanes **13**[10] (upper) and **14** (lower). Primed and unprimed atoms are related by crystallographically imposed centrosymmetry. In addition, **14** has an imposed mirror plane containing the bridge rhomb Fe1Fe1′S3S3′. Selected mean bond distances (Å) and angles (deg) are indicated. The shorter Fe−S distances are mean values involving S1, S2, S3 (**13**) or S1, S2 (**14**) and the longer values involved S4 (**13**) or S3 (**14**).

of 2.225(2) Å in **14** ($Fe^{2.33+}$) is on the long end of values for an $[Fe_4S_4]^{2+}$ cluster; the difference in terminal Fe−SR distances in clusters differing by two electrons ($[Fe_4S_4]^{+,3+}$) is ca.0.1 Å.[26] Evidently, oxidation results in the depopulation of antibonding orbitals with substantial Fe−S character.

Summary. The following are the principal results and conclusions of this investigation and include observations from prior research.[10,11]

(1) The edge-bridged double cubane **2** undergoes two types of reactions with conservation of nuclearity: terminal ligand substitution with retention of core structure, and core rearrangement to the P^N-type cluster topology. Edge-bridged double cubanes have been obtained in the all-ferrous $[Mo_2Fe_6S_8]^{2+}$ (**4**, **9**, **13**), $[Mo_2Fe_6S_8]^{3+}$ (**6**), and $[Mo_2Fe_6S_8]^{4+}$ (**12**, **14**) oxidation states.

(2) Edge-bridged double cubanes can be converted to P^N-type clusters by four distinct processes (minimal reactions 2−5) and are stabilized by terminal thiolate (**3**, **7**, **8**) or methoxide ligands with one (**10**) or two (**11**) methoxide bridges. These clusters possess idealized C_{2v} core symmetry (excluding **10**). The stable oxidation state is $[Mo_2Fe_6S_9]^+$.

(3) A P^N-type cluster (**10**) can be converted to edge-bridged double cubanes (**12**, **14**; reaction 7 followed by oxidation). A reversible transformation between the two structure types (e.g., bidirectional reaction 3) has not been observed.

(4) As the designation implies, P^N-type clusters simulate the $Fe_8S_7(\mu_2\text{-}S_{Cys})_2 = Fe_8(\mu_2\text{-}S)_2(\mu_3\text{-}S)_6(\mu_6\text{-}S)$ core of the nitrogenase P^N cluster. Best-fit superpositions of the core structures of the native and synthetic clusters yield the following weighted rms deviations in atom positions: 0.38 (**3**), 0.31 (**7**), 0.22 (**10**), 0.20 Å (**11**).[27] A brief comparison of specific metric parameters is available in Table 3.

The investigation and those preceding it[10,11] provide a comprehensive account of the synthesis of structural analogues of the nitrogenase P^N cluster and the synthesis, structures and reactions of edge-bridged double cubanes. In our hands thus far, the P^N topology is synthetically accessible only from double cubane precursors. It is a matter of considerable interest that the system $8[Fe(N(SiMe_3)_2]/3(Me_2N)_2CS/12$ 2,4,6-$Pr^i_3C_6H_2SH/7S$ yields the cluster $[Fe_8S_7(\mu_2\text{-}N(SiMe_3)_2)_2((Me_2N)_2CS)_2(N(SiMe_3)_2)_2]$ with an $Fe_8(\mu_3\text{-}S)_6(\mu_6\text{-}S)$ core fragment similar to that of the native cluster. At present, we do not perceive a relationship between this example of cluster self-assembly and the core rearrangement reactions set out here for the synthesis of the P^N-cluster topology. Our continuing investigation of weak-field clusters related to the native clusters of nitrogenase utilizes single and double cubanes and P^N-type clusters as reactants in cluster synthesis and builds upon the findings reported here.

Acknowledgment. This research was supported by NIH Grant GM 28856.

Supporting Information Available: X-ray crystallographic data in CIF format for the 10 compounds in Table 1. This material is available free of charge via the Internet at http://pubs.acs.org.

IC030259T

(27) For examples of best-fit superposition diagrams, cf. refs 3 and 10 and: Lee, S. C.; Holm, R. H. *Chem. Rev.*, posted on Nov 6, 2003, http://pubs.acs.org, cr0206216.